

# Isotopic Production Cross Section Updates in GALPROP for Supporting TIGERISS

**P. Ghosh<sup>a,b,c</sup>,\* I. V. Moskalenko<sup>d</sup>, T. Porter<sup>d</sup>, J. F. Krizmanic<sup>a</sup> and the TIGERISS Collaboration**

(a complete list of authors can be found at the end of the proceedings)

<sup>a</sup>*NASA Goddard Space Flight Center, Astrophysics Science Division,  
9432 Greenbelt Rd, Greenbelt, MD 20771, USA*

<sup>b</sup>*Catholic University of America,  
620 Michigan Ave NE, Washington DC 20064, USA*

<sup>c</sup>*Center for Research and Exploration in Space Sciences and Technology II,*

<sup>d</sup>*Stanford University,  
450 Serra Mall, Stanford, CA 94305, USA*

*E-mail:* [priyarshini.ghosh@nasa.gov](mailto:priyarshini.ghosh@nasa.gov)

The PIONEERS-selected mission TIGERISS, planned to launch to the ISS in 2026, will provide, for the first time, single-element resolution galactic cosmic-ray elemental abundance spanning the periodic table, from  $^5\text{B}$  up to  $^{82}\text{Pb}$ , to further our understanding of the grand cycle of matter in the galaxy. Such wide-range, fine-resolution experimental data would be best combined with the latest developments in astrophysical models, but the current accuracy of nuclear isotopic production cross sections is far behind experimental data, so GALPROP is updating its current cross section library with newer reaction channels and more accurate data on existing channels that have been reported over the last two decades, enabling one to obtain a better understanding of the galactic chemical composition. The main focus of reaction channels are proton spallation reactions of 1) isotopes of  $^5\text{B}$  through  $^{82}\text{Pb}$ , and 2) the sub-Fe group, because recent studies have indicated that improvements in spallation cross section data are required to use the electron-capture cosmic rays for constraining geometric properties of diffusion models.

POS (ICRC2023) 049

*38th International Cosmic Ray Conference (ICRC2023)*  
26 July - 3 August, 2023  
Nagoya, Japan



\*Speaker

© Copyright owned by the author(s) under the terms of the Creative Commons Attribution-NonCommercial-NoDerivatives 4.0 International License (CC BY-NC-ND 4.0).

<https://pos.sissa.it/>

## 1. Introduction

Galactic Cosmic Rays (GCRs) carry information about how the galaxy produces and distributes different elements, and they are one of the few direct samples of matter from outside the solar system. Excellent elemental abundance data up to  $Z = 30$  are presently available from various instruments, such as ACE-CRIS [1], AMS-02 [2-7], CALET [8-10], etc. For  $30 < Z < 60$ , results from TIGER [11] and SuperTIGER [12] must be combined with measured data from missions such as HEAO-HNE and ACE-CRIS to clearly show continuous separation of refractory and volatile elements. For  $Z > 60$ , the Trek [13] detector on MIR has measured the only existing data with single element resolution at the highest charges, but are almost impossible to normalize, given the lack of other comparable measurements and Trek's sensitivity to  $Z > \sim 70$ . Thus, the relative rarity of GCRs at higher charges makes Ultra-Heavy GCR (UHGCR) individual elemental abundances above nuclear charge  $Z = 56$  difficult to measure and remain unknown.

The Trans-Iron Galactic Element Recorder for the International Space Station (TIGERISS) will address the scarcity of UHGCR data in several ways [14]. Firstly, by combining Silicon Strip Detectors and Cherenkov detectors, TIGERISS will be able to measure charge with uncertainty on the order of 0.2 charge units from  ${}^5\text{B}$  up to  ${}^{82}\text{Pb}$  (Fig. 1). This unprecedented fine resolution for the UHGCR range will allow TIGERISS to separate abundant even-charged nuclei from rarer odd-charged nuclei. Additionally, the wide range of measurement from a single instrument enables normalization that resolves discrepancies between previous instruments, such as that of ACE-CRIS and SuperTIGER/CALET. Lastly, TIGERISS will have lesser systematic uncertainties in its results, primarily due to the lack of atmospheric overburden on the ISS.

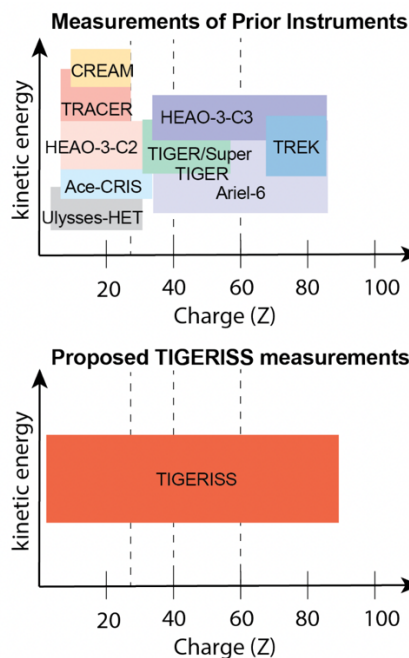


Figure 1: TIGERISS will be the first instrument to measure UHGCR abundances from B to Pb with single-element resolution, thus eliminating the need for normalization with other measurements.

Equipped with such first-of-its-kind capabilities, TIGERISS aims to provide insight into astrophysical nucleosynthesis; specifically, to address questions about the origins of r-process nuclei and the contributions of these origins to the galactic r-process budget, and the limits of CR nucleosynthesis and acceleration in OB associations. Our understanding of the galactic composition and GCR propagation has come a long way since the advent of analytical and semi-analytical techniques, and with the continuous flow of new and more accurate data from space, balloon and ground-based measurements, there is a need for models that incorporate the complexities of propagation of GCRs. To model such complex phenomena, the numerical code GALPROP [15] calculates the propagation of relativistic charged particles and the diffuse emissions produced during their propagation. The code includes astrophysical models as realistic as possible with the latest theoretical developments. GALPROP works by calculating the propagation of cosmic-ray nuclei, antiprotons, electrons and positrons, and computes diffuse  $\gamma$ -rays and synchrotron emission in the same framework. While the experimental data from TIGERISS will enable GALPROP to better constrain its models, the accuracy in interpreting observed CR data is dependent on the accuracy of cross-section (CS) data available, which becomes a bottleneck in identifying the subtle features of galactic phenomenon, thereby necessitating a careful and continual updating of CS data in models.

## 1.1 Updating Cross Sections in GALPROP

There are over 2,000 cross sections in GALPROP's current library [16] for proton spallation reactions, spanning approximately 176 reaction channels up to  $Z = 30$ , with the data being sourced from various sources between 1950 and 1999. Since then, many new experiments have been performed, with newly measured reaction channels, and more accurate cross-section data on existing channels. Given TIGERISS' capability of measuring elemental abundance till  $_{82}\text{Pb}$ , there is an ongoing effort to add high  $Z$  spallation reactions above  $Z = 30$ . Furthermore, [17] and [18] have repeatedly hypothesized, based on the continued inconsistencies between observations of the  $^{51}\text{V}/^{51}\text{Cr}$  and  $^{49}\text{Ti}/^{49}\text{V}$  ratios, that the inconsistencies are a result of large uncertainties in existing fragmentation cross sections. In fact, [19, 20] postulated that reducing the  $^{49}\text{Ti}$  fragmentation cross-section by 15% would resolve the discrepancy. Therefore, the other area of interest is the electron-capture isotopes in the sub-Fe group that can be used to study energy-dependent propagation, such as diffusive reacceleration in the ISM and heliospheric modulation.

### 1.1.1 Methodology of Data Selection

Numerous experiments report CS data for reactions; some add to previously existing data and reaction channels, some report completely new reactions. Comprehensive lists of CS data are extracted from libraries such as ENDF, EXFOR, the Landolt-Börnstein series, from experiments performed all over the world, such as at GSI in Dermstadt, Germany, the Bevatron at Lawrence Berkeley Laboratory in California, USA, the Clinton P. Anderson Meson Physics Facility at Los Alamos National Laboratory in New Mexico, USA, amongst many others. It would be an overwhelming task to gather data from the large number of sources online, therefore it is imperative to have a systematic sorting of data, so the appropriate measurements can be selected. Several parameters determine the limitations of the CS data and their relevancy for our purposes. Below, are certain parameters that help us decide which data to select and which to discard:

1. Cross section type: Individual (the probability of a nuclear interaction resulting in a daughter nuclide only), cumulative (a sum of cross sections of all reaction channels on a well-defined target nucleus, which lead to direct production of the final nuclide), decayed (the same final nuclide can also be produced indirectly via the decay of progenitors produced simultaneously on the target nucleus), metastable states (decayed daughter isotopes in isomeric states versus in ground states), charge-changing (when the reaction results in a change of charge  $Z$ ), mass-changing (when the reaction results in a change of mass  $A$ ). Data with different types of cross sections cannot be lumped together.
2. Type of experiment performed: Direct and reverse kinematics. In direct kinematic experiments, heavy projectiles are accelerated to cosmic-ray velocities, representing the primary cosmic ray nucleus, and are bombarded on a stationary hydrogen target representing the interstellar medium (ISM), such as a liquid H target. While this type of interaction is an exact representation of cosmic-ray interaction in the ISM, the safety and maintenance costs of liquid H are prohibitively high, or target subtractions are necessary if  $\text{CH}_4$  targets are used instead. The solution to this dilemma is to use reverse kinematics, where the assumption is made that the ISM is mostly hydrogen, and hence a ‘moving’ ISM (proton beam) is accelerated towards a fixed cosmic ray (nuclear target). Although this setup is much simpler and cost-effective, the method assumes no collective effect in the target including molecular effects, and it is the reverse of how CR interactions take place in the ISM. The type of experiment performed can have a strong bearing on the errors reported, thereby dictating the relevancy of the experimental data to be included.
3. Uncertainty: Errors can be of the systematic kind (determined by factors such as beam purity, intensity fluctuations, target purity, spectrometer calibration, detector efficiency, self-absorption of  $\gamma$ -rays in sample, interference from secondary particles) or statistical (determined by lower cross sections, detector count rates, correction of unresolved  $\gamma$ -lines, background under spectral peak, spectrometer dead time and count loss, total error of the nuclide production rate, etc.)

If a reaction channel has both individual and cumulative cross section data, they are not used together but are separately cross-checked. Many reactions have resonance features at lower energies, typically below 100 MeV/nucleon, so they are eliminated from analysis by setting a lower energy bound for each reaction channel.

Previously, attention had not been paid to lower-energy CS, i.e.,  $< 100$  MeV/nucleon, but they have garnered interest in recent years, because, earlier there wasn’t much data available outside of the heliosphere and the modulation potential was 400 MV at minimum, but there now exists data from ISM where low-energy particles can be measured. Secondly, simpler propagation models like Leaky Box featured simple diffusion models without energy gain; but now with complex models that include diffusion and re-acceleration and other intricate processes in the ISM, low-energy particles can gain energy and so low-energy cross section behaviour becomes important.

Once the appropriate CS data has been selected, they are then parametrized into continuous cross-section data across the energy range of interest using several schemes such as

re-normalized fits of Silverberg and Tsao's code or Webber's code (according to their energy range of validity), empirical fits based on available data, and on theoretical calculations.

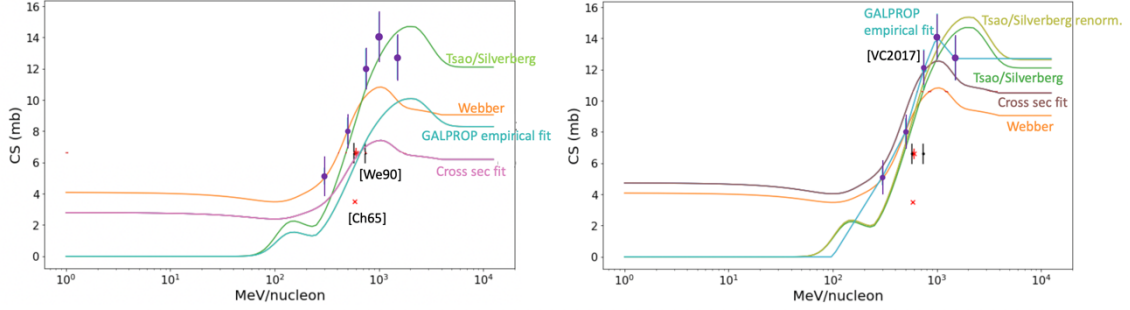


Figure 2. Parameterization for  $^{56}\text{Fe} + p \rightarrow 40\text{K}$  in GALPROP using (left) older data, and (right) newer, more accurate data.

In Fig. 2 is shown the cross section parametrization for the reaction  $^{56}\text{Fe} + p \rightarrow 40\text{K}$ . On the left is the parametrization fits and schemes for older data of cumulative cross sections from [Ch65] which reported no uncertainty, and from [We90] whose beam purity was not reported with well-defined systematic uncertainty. Webber and Silverberg/Tsao's don't agree well with the few data points, the cross-section as well as the GALPROP fits do not follow data trends, either. The figure on the right shows the parametrization using newer data from [VC2017], which are individual cross sections, and have very well-defined error bars. The cross section fit miss the highest two data points from [VC2017], Tsao/Silverberg's fit matches closer with the data than Webber's, and GALPROP's empirical fit is used to pass through the data points.

Finally, Fig. 3 shows the current status of reaction channels in GALPROP's CS library. Green pixels represent reaction channels that are already present in v57 version of GALPROP that is available online. Red pixels represent reaction channels that are present in the v57 version, but newer, more accurate data has been made available for the existing channel and are being incorporated into the library. Yellow pixels represent completely new reaction channels. This is an ongoing effort and there are many more reaction channels to be added, which will be available online on the next version. Efforts are ongoing to add more reaction channels to the sub-Fe group and  $Z > 30$ .

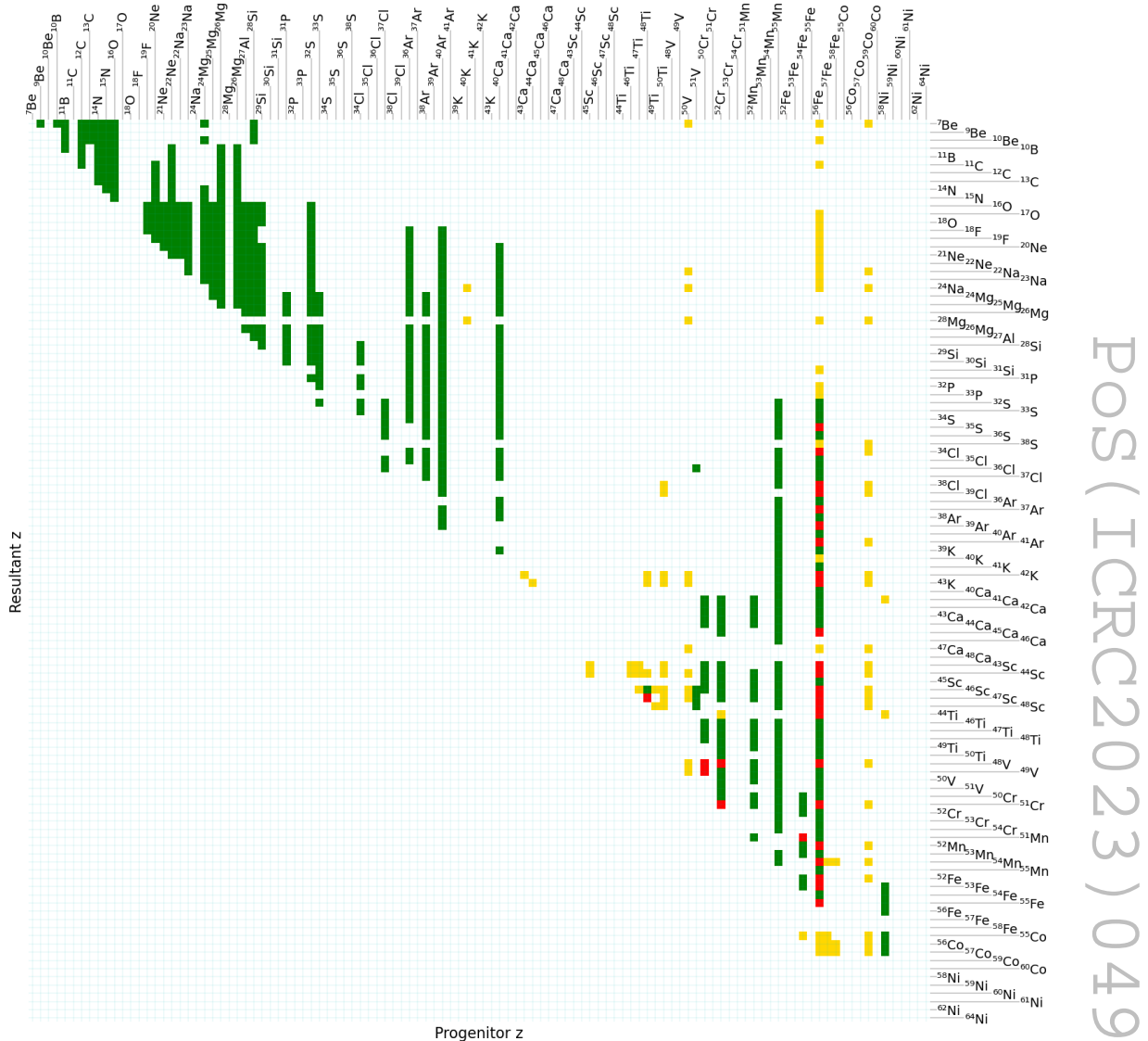


Figure 3. Reaction channels for proton spallation of elements.

## References

- [1] K. A. Lave et al., "GALACTIC COSMIC-RAY ENERGY SPECTRA AND COMPOSITION DURING THE 2009- 2010 SOLAR MINIMUM PERIOD," *ApJ*, vol. 770, no. 2, p. 117, Jun. 2013, doi: 10.1088/0004- 637X/770/2/117
- [2] M. Aguilar et al., "ISOTOPIC COMPOSITION OF LIGHT NUCLEI IN COSMIC RAYS: RESULTS FROM AMS-01," *ApJ*, vol. 736, no. 2, p. 105, Aug. 2011, doi: 10.1088/0004- 637X/736/2/105
- [3] M. Aguilar et al., "Properties of Cosmic Helium Isotopes Measured by the Alpha Magnetic Spectrometer," *Phys. Rev. Lett.*, vol. 123, no. 18, p. 181102, Nov. 2019, doi: 10.1103/PhysRevLett.123.181102

- [4] M. Aguilar et al., “Properties of a New Group of Cosmic Nuclei: Results from the Alpha Magnetic Spectrometer on Sodium, Aluminum, and Nitrogen,” *Phys. Rev. Lett.*, vol. 127, no. 2, p. 021101, Jul. 2021, doi: 10.1103/PhysRevLett.127.021101
- [5] M. Aguilar et al., “Precision Measurement of the Boron to Carbon Flux Ratio in Cosmic Rays from 1.9 GV to 2.6 TV with the Alpha Magnetic Spectrometer on the International Space Station,” *Phys. Rev. Lett.*, vol. 117, no. 23, p. 231102, Nov. 2016, doi: 10.1103/PhysRevLett.117.231102.
- [6] M. Aguilar et al., “Properties of Heavy Secondary Fluorine Cosmic Rays: Results from the Alpha Magnetic Spectrometer,” *Phys. Rev. Lett.*, vol. 126, no. 8, p. 081102, Feb. 2021, doi: 10.1103/PhysRevLett.126.081102
- [7] M. Aguilar et al., “Properties of Iron Primary Cosmic Rays: Results from the Alpha Magnetic Spectrometer,” *Phys. Rev. Lett.*, vol. 126, no. 4, p. 041104, Jan. 2021, doi: 10.1103/PhysRevLett.126.041104
- [8] O. Adriani et al., “Direct Measurement of the Cosmic-Ray Proton Spectrum from 50 GeV to 10 TeV with the Calorimetric Electron Telescope on the International Space Station,” *Phys. Rev. Lett.*, vol. 122, no. 18, p. 181102, May 2019, doi: 10.1103/PhysRevLett.122.181102.
- [9] O. Adriani et al., “Direct Measurement of the Cosmic-Ray Carbon and Oxygen Spectra from 10 GeV / n to 2.2 TeV / n with the Calorimetric Electron Telescope on the International Space Station,” *Phys. Rev. Lett.*, vol. 125, no. 25, p. 251102, Dec. 2020, doi: 10.1103/PhysRevLett.125.251102.
- [10] O. Adriani et al., “Measurement of the Iron Spectrum in Cosmic Rays from 10 GeV / n to 2.0 TeV / n with the Calorimetric Electron Telescope on the International Space Station,” *Phys. Rev. Lett.*, vol. 126, no. 24, p. 241101, Jun. 2021, doi: 10.1103/PhysRevLett.126.241101.
- [11] B. F. Rauch et al., “COSMIC RAY ORIGIN IN OB ASSOCIATIONS AND PREFERENTIAL ACCELERATION OF REFRactory ELEMENTS: EVIDENCE FROM ABUNDANCES OF ELEMENTS 26 Fe THROUGH 34 Se,” *ApJ*, vol. 697, no. 2, pp. 2083–2088, Jun. 2009, doi: 10.1088/0004-637X/697/2/2083.
- [12] R. P. Murphy et al., “GALACTIC COSMIC RAY ORIGINS AND OB ASSOCIATIONS: EVIDENCE FROM SuperTIGER OBSERVATIONS OF ELEMENTS 26 Fe THROUGH 40 Zr,” *ApJ*, vol. 831, no. 2, p. 148, Nov. 2016, doi: 10.3847/0004-637X/831/2/148.
- [13] A. J. Westphal, P. B. Price, B. A. Weaver, and V. G. Afanasiev, “Evidence against stellar chromospheric origin of Galactic cosmic rays,” *Nature*, vol. 396, no. 6706, pp. 50–52, Nov. 1998, doi: 10.1038/23887.
- [14] N. E. Walsh, “PhD. Thesis: SuperTIGER Elemental Abundances for the Charge Range  $41 \leq Z \leq 56$ ,” Washington University, 2020.
- [15] A.W. Strong, I.V. Moskalenko, “Models for galactic cosmic-ray propagation”, *Advances in Space Research*, Volume 27, Issue 4, 2001, Pages 717-726, ISSN 0273-1177.
- [16] Moskalenko, Igor & Jóhannesson, Gudlaugur & Orlando, Elena & Porter, Troy & Strong, A.W.. (2017). GALPROP Code for Galactic Cosmic Ray Propagation and Associated Photon Emissions. 279. 10.22323/1.301.0279.
- [17] F. C. Jones, A. Lukasiak, V.S. Ptuskin, W.R. Webber, K-capture cosmic ray secondaries and reacceleration, *Advances in Space Research*, Volume 27, Issue 4, 2001, Pages 737-741, ISSN 0273-1177, [https://doi.org/10.1016/S0273-1177\(01\)00113-2](https://doi.org/10.1016/S0273-1177(01)00113-2).
- [18] Niebur S. M., Binns W. R., Christian E. R. *et al.* 2001 *Proc. ICRC (Hamburg)* **5** 1675
- [19] Niebur, S. M., et al. (2003), Cosmic ray energy loss in the heliosphere: Direct evidence from electron-capture-decay secondary isotopes, *J. Geophys. Res.*, 108, 8033, doi:[10.1029/2003JA009876](https://doi.org/10.1029/2003JA009876), A10.

[20] Benyamin D., Shaviv N.J., and Piran T. (2017). Electron-capture Isotopes Could Constrain Cosmic-Ray Propagation Models. *The Astrophysical Journal*, vol. 851, pp.109 -115.

Full Author:

R. F. Borda<sup>1</sup>, R. G. Bose<sup>2</sup>, D. L. Braun<sup>2</sup>, J. H. Buckley<sup>2</sup>, J. Calderon<sup>3</sup>, N. W. Cannady<sup>1,4,5</sup>, R. M. Caputo<sup>4</sup>, S. Coutu<sup>6</sup>, G. A. de Nolfo<sup>7</sup>, P. Ghosh<sup>8,4,5</sup>, S. Jones<sup>3</sup>, C. A. Kierans<sup>4</sup>, J. F. Krizmanic<sup>4</sup>, W. Labrador<sup>2</sup>, L. Lisalda<sup>2</sup>, J. V. Martins<sup>1</sup>, M. P. McPherson<sup>9</sup>, E. Meyer<sup>1</sup>, J. Mitchell<sup>7</sup>, J. W. Mitchell<sup>4</sup>, S. I. Mognet<sup>6</sup>, A. Moiseev<sup>10,4,5</sup>, S. Nutter<sup>3</sup>, I. Pastrana<sup>2</sup>, B. F. Rauch<sup>2</sup>, H. Salmani<sup>9</sup>, M. Sasaki<sup>10,4,5</sup>, G. E. Simburger<sup>2</sup>, S. Smith<sup>9</sup>, H. A. Tolentino<sup>9</sup>, D. Washington<sup>6</sup>, W. V. Zober<sup>2</sup>

<sup>1</sup>University of Maryland, Baltimore County,

<sup>2</sup>Department of Physics and McDonnell Center for the Space Sciences, Washington University in St. Louis,

<sup>3</sup>Northern Kentucky University,

<sup>4</sup>NASA Goddard Space Flight Center, Astrophysics Science Division,

<sup>5</sup>Center for Research and Exploration in Space Sciences and Technology II,

<sup>6</sup>Pennsylvania State University,

<sup>7</sup>NASA Goddard Space Flight Center, Heliophysics Science Division,

<sup>8</sup>Catholic University of America,

<sup>9</sup>Howard University,

<sup>10</sup>University of Maryland, College Park